

energy of fragments and ejected liquid is not subtracted from blast energy. This may produce an error of up to 50%, which translates into an overstatement of overpressure by 25%. (See Section 6.3.1.4.)

In practice, vapor release will not be spherical, as is assumed in the method. A release from a cylinder burst may produce overpressures along the vessel's axis, which are 50% lower than pressures along a line normal to its axis. If a vessel ruptures from ductile, rather than brittle, fracture, a highly directional shock wave is produced. Overpressure in the other direction may be one-fourth as great. The influences of release direction are not noticeable at great distances. Uncertainties for a BLEVE are even higher because of the fact that its overpressure is limited by initial peak-shock overpressure is not taken into account.

The above methods assume that all superheated liquids can flash explosively, yet this may perhaps be the case only for liquids above their superheat-limit temperatures or for pre-nucleated fluids. Furthermore, the energies of evaporating liquid and expanding vapor are taken together, while in practice, they may produce separate blasts. Finally, in practice, there are usually structures in the vicinity of an explosion which will reflect blast or provide wind shelter, thereby influencing the blast parameters.

In practice, overpressures in one case might very well be only one-fifth of those predicted by the method and close to the predicted value in another case. This inherent inaccuracy limits the value of this method in postaccident analysis. Even when overpressures can be accurately estimated from blast damage, released energy can only be estimated within an order of magnitude.

6.4. FRAGMENTS

A BLEVE can produce fragments that fly away rapidly from the explosion source. These primary fragments, which are part of the original vessel wall, are hazardous and may result in damage to structures and injuries to people. Primary missile effects are determined by the number, shape, velocity, and trajectory of fragments.

When a high explosive detonates, a large number of small fragments with high velocity and chunky shape result. In contrast, a BLEVE produces only a few fragments, varying in size (small, large), shape (chunky, disk-shaped), and initial velocities. Fragments can travel long distances, because large, half-vessel fragments can "rocket" and disk-shaped fragments can "frisbee." The results of an experimental investigation described by Schulz-Forberg et al. (1984) illustrate BLEVE-induced vessel fragmentation.

All parameters of interest with respect to fragmentation will be discussed. The extent of damage or injury caused by these fragments is, however, not covered in this volume. (Parameters of the terminal phase include first, fragment density and velocity at impact, and second, resistance of people and structures to fragments.)

Figure 6.32 illustrates results of three fragmentation tests of 4.85-m³ vessels 50% full of liquid propane. The vessels were constructed of steel (StE 36; unalloyed

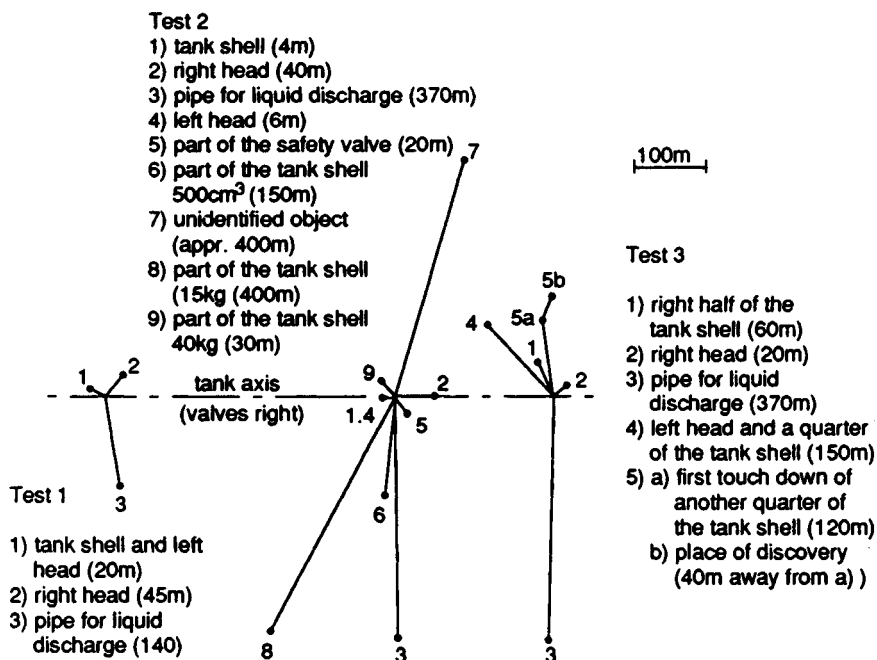


Figure 6.32. Schematic view of vessel fragments' flight after vessel bursts in three BLEVE tests (Schulz-Forberg et al. 1984).

fine-grained steel with a minimum yield strength of 360 N/mm²), and had wall thicknesses of 5.9 mm (Test 1) and 6.4 mm (Tests 2 and 3). Vessel overpressure at moment of rupture was 24.5 bar in the first test, 39 bar in the second test, and 30.5 bar in the third.

Research on predictions of fragment velocity and range has heretofore been concentrated on the idealized situation of the gas-filled, pressurized vessel. Other cases, including those of nonideal gas-filled vessels and vessels containing combinations of gas and liquid, are now being investigated (Johnson et al. 1990). Fragment velocity and range can be assumed to depend on the total available energy of a vessel's contents. If this energy is known, the vessel's contents are not significant. It is, therefore, permissible to begin by describing the effects of a vessel rupture when filled with an ideal gas.

6.4.1. Initial Fragment Velocity for Ideal-Gas-Filled Vessels

6.4.1.1. Estimate Based on Total Kinetic Energy

A theoretical upper limit of initial fragment velocity can be calculated if it is assumed that the total internal energy E of the vessel contents is translated into

fragment kinetic energy. Two simple relations are obtained:

$$v_i = \left[\frac{2E_k}{M} \right]^{1/2} \quad (6.4.1)$$

where

$$\begin{aligned} v_i &= \text{initial fragment velocity} && (\text{m/s}) \\ E_k &= \text{kinetic energy} && (\text{J}) \\ M &= \text{total mass of the empty vessel} && (\text{kg}) \end{aligned}$$

Kinetic energy (E_k) is calculated from internal energy E . Internal energy can be calculated from [similar to Eq. (6.3.2)]:

$$E = \frac{(p_1 - p_0)V}{\gamma - 1} \quad (6.4.2)$$

in which

$$\begin{aligned} p_1 &= \text{absolute pressure in vessel at failure} && (\text{N/m}^2) \\ p_0 &= \text{ambient pressure outside vessel} && (\text{N/m}^2) \\ V &= \text{internal volume of vessel} && (\text{m}^3) \\ \gamma &= \text{ratio of specific heats} && (-) \end{aligned}$$

This equation was first proposed by Brode (1959).

In accidental releases, pressure within a vessel at time of failure is not always known. However, depending on the cause of vessel failure, an estimate of its pressure can be made. If failure is initiated by a rise in initial pressure in combination with a malfunctioning or inadequately designed pressure-relief device, the pressure at rupture will equal the vessel's failure pressure, which is usually the maximum allowable working pressure times a safety factor. For initial calculations, a usual safety factor of four can be applied for vessels made of carbon steel, although higher values are possible. (The higher the failure pressure, the more severe the effects.)

If failure is due to fire exposure, the vessel's overpressure results from external overheating and can reach a maximal value of 1.21 times the opening pressure of the safety valve. This maximal value is called the accumulated pressure. As overheating reduces the vessel's wall strength, failure occurs at the point at which its strength is reduced to a level at which the accumulated pressure can no longer be resisted. If vessel failure is due to corrosion or impact, it can be assumed that pressure at failure will be the operating pressure.

Application of Eqs. (6.4.1) and (6.4.2) produce a large overestimation of the initial velocity v_i . As a result, refinements were developed in the methods for determining energy E . For a sudden rupture of a vessel filled with an ideal gas, decompression will occur so rapidly that heat exchange with surroundings will be negligible. Assuming adiabatic expansion, the highest fraction of energy available for translation to kinetic energy of fragments can be calculated with:

$$E = kp_1V/(\gamma - 1) \quad (6.4.3)$$

where

$$k = 1 - \left[\frac{p_0}{p_1} \right]^{(\gamma-1/\gamma)} \quad (6.4.4)$$

(See Baker 1973.) Equation (6.4.4) is explained in Section 6.3.1.1. Baum (1984) has refined this equation by incorporating the work of air pushed away by expanding gas:

$$k = 1 - \left[\frac{p_0}{p_1} \right]^{(\gamma-1/\gamma)} + (\gamma - 1) \frac{p_0}{p_1} \left[1 - \left(\frac{p_0}{p_1} \right)^{-1/\gamma} \right] \quad (6.4.5)$$

For pressure ratios p_1/p_0 from 10 to 100 and γ ranges from 1.4 to 1.6, the factor k varies between 0.3 and 0.6, according to the refined equation proposed by Baum (1984). These refinements can reduce the calculated value of v_1 by about 45%. According to Baum (1984) and Baker et al. (1978b), the kinetic energy calculated with the above equations is still an upper limit.

In Baum (1984), the fraction of total energy translated into kinetic energy is derived from data on fragment velocity measured in a large variety of experiments. (The experiments applied for this purpose include those described by Boyer et al. 1958; Boyer 1959; Glass 1960; Esparza and Baker 1977a; Moore 1967; Collins 1960; Moskowitz 1965; and Pittman 1972.) From these experiments, the fraction translated to kinetic energy was found to be between 0.2 to 0.5 of the total energy derived through Baum's refinement.

Based on these figures, it is appropriate to use $k = 0.2$ in the equation:

$$E_k = kp_1V/(\gamma - 1) \quad (6.4.6)$$

for rough initial calculations.

6.4.1.2. Initial Velocity Based on Theoretical Considerations

A great deal of theoretical work has been performed to improve ability to predict initial fragment velocity. In the course of these efforts, a model introduced by Grodzovskii and Kukanov (1965) has been improved by various investigators. In this model, the acceleration force on fragments is determined by taking into account gas flow through ever-increasing gaps between fragments. This approach recognizes that not all available energy is translated to kinetic energy. Hence, calculated initial velocities are reduced.

Velocities of fragments from spherical pressure vessels bursting into two equal portions have been analytically determined for ideal gases by the work of Taylor and Price (1971). The theory was expanded to include a large number of fragments by Bessey (1974) and to cylindrical geometries by Bessey and Kulesz (1976). Baker et al. (1978b) modified the theory for unequal fragments. In calculations of initial velocity, the energy necessary to break vessel walls is neglected.

Baker et al. (1975) compare computer-code predictions of fragment velocity from spheres bursting into a large number of pieces and with some experimental

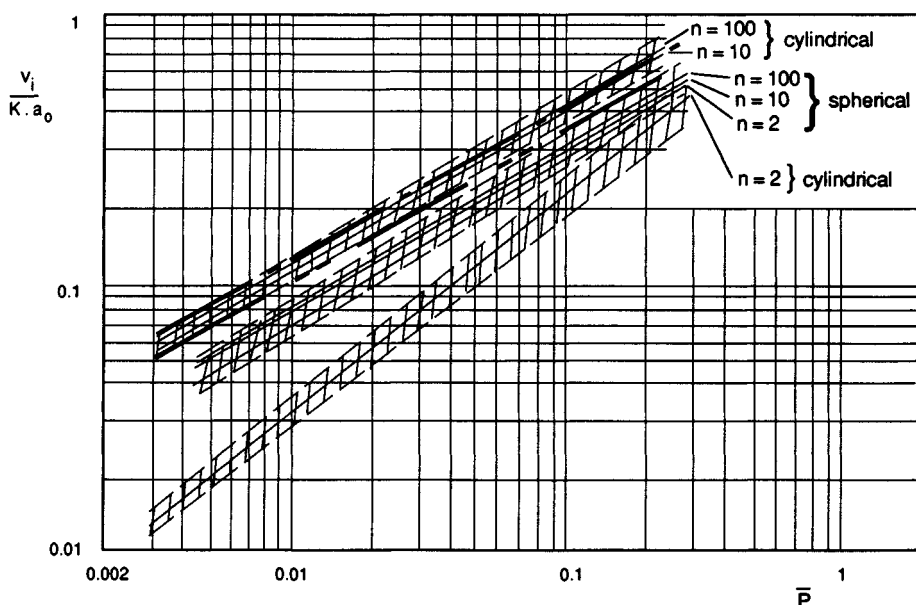


Figure 6.33. Fragment velocity versus scaled pressure. (— · — · — ·): spheres according to $v_i = 0.88a_0 F^{0.55}$ [Eq. (6.4.15)]. (— · — · — ·): cylinders according to $v_i = 0.88a_0 F^{0.55}$ [Eq. (6.4.15)]. (From Baker et al. 1983.)

data. Boyer et al. (1958) and Pittman (1972) measured fragment velocities from bursting glass spheres and bursting titanium alloy spheres, respectively. The calculated and measured velocities agree rather well after reported difficulties in velocity measurement are taken into account.

The results of a parameter study were used to compose a diagram (Figure 6.33) which can be used to determine initial fragment velocity (Baker et al. 1978a and 1983).

Figure 6.33 can be used to calculate the initial velocity v_i for bursting pressurized vessels filled with ideal gas. The quantities to be substituted, in addition to those already defined (p_1 , p_0 , and V), are

a_0	= speed of sound in gas at failure	(m/s)
M	= mass of vessel	(kg)
K	= factor for unequal fragments	(—)
\bar{p}	= scaled pressure	(—)

with

$$\bar{p} = (p_1 - p_0)V/(Ma_0^2) \quad (6.4.7)$$

Separate regions in Figure 6.33 account for scatter of velocities of cylinders and spheres separating into 2, 10, or 100 fragments. The assumptions used in deriving the figure are from Baker et al. (1983), namely,

- The vessel under gas pressure bursts into equal fragments. If there are only two fragments and the vessel is cylindrical with hemispherical end-caps, the vessel bursts perpendicular to the axis of symmetry. If there are more than two fragments and the vessel is cylindrical, strip fragments are formed and expand radially about the axis of symmetry. (The end caps are ignored in this case.)
- Vessel thickness is uniform.
- Cylindrical vessels have a length-to-diameter ratio of 10.
- Contained gases used were hydrogen (H_2), air, argon (Ar), helium (He), or carbon dioxide (CO_2).

The sound speed a_0 of the contained gas has to be calculated for the temperature at failure:

$$a_0^2 = T\gamma R/m \quad (6.4.8)$$

where

a_0	= speed of sound	(m/s)
R	= ideal gas constant	(J/Kkmol)
T	= absolute temperature inside vessel at failure	(K)
m	= molecular mass	(kg/kmol)

Appendix D gives some specific characteristics for common gases.

When using Figure 6.33, for equal fragments, K has to be taken as 1 (unity). For the case of a cylinder breaking into two unequal parts perpendicular to the cylindrical axis, K was calculated by Baker et al. (1983). Factor K can be determined for a fragment with mass M_f with the aid of Figure 6.34. The dotted lines in the figure bound the scatter region.

Figure 6.34 indicates that heavier fragments will have higher initial velocities. Whether factor K is correct is doubtful. In Baker et al. (1978b), another figure for the determination of K was presented that gives totally different values. No explanation for the discrepancy has been found. It is, therefore, advisable to use $K = 1$ only.

6.4.1.3. Initial Velocity Based on Empirical Relations

In addition to the theoretically derived Figure 6.33, an empirical formula developed by Moore (1967) can also be used for the calculation of the initial velocity:

$$v_i = 1.092 \left[\frac{EG}{M} \right]^{0.5} \quad (6.4.9)$$

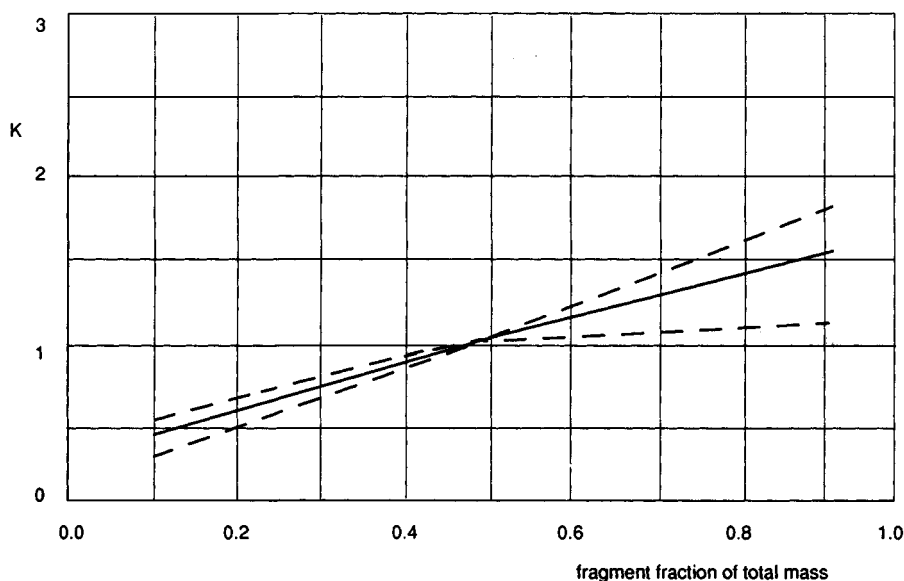


Figure 6.34. Adjustment factor for unequal mass fragments (Baker et al. 1983).

where for spherical vessels

$$G = \frac{1}{1 + 3C/5M}$$

and for cylindrical vessels

$$G = \frac{1}{1 + C/2M}$$

where

C = total gas mass (kg)

E = energy (J)

M = mass of casing or vessel (kg)

Moore's equation was derived for fragments accelerated from high explosives packed in a casing. The equation predicts velocities higher than actual, especially for low vessel pressures and few fragments. According to Baum (1984), the Moore equation predicts velocity values between the predictions of the equations given at the beginning of this section and the values derived from Figure 6.33.

Other empirical relations for ideal gas are given in Baum (1987); recommended velocities are upper limits. In each of these relations, a parameter F has been applied.

For a large number of fragments, F is given by:

$$F = \frac{(p_1 - p_0)r}{ma_0^2} \quad (6.4.10)$$

where m is mass per unit area of vessel wall and r the radius of the vessel. For a small number of fragments, F can be written as:

$$F = \frac{(p_1 - p_0)Ar}{M_f a_0^2} \quad (6.4.11)$$

where

$$\begin{aligned} r &= \text{radius of vessel} & (\text{m}) \\ A &= \text{area of detached portion of vessel wall} & (\text{m}^2) \\ M_f &= \text{mass of fragment} & (\text{kg}) \end{aligned}$$

From these values of F , the following empirical relations for initial velocity have been derived:

- For an end-cap breaking from a cylindrical vessel:

$$v_i = 2a_0 F^{0.5} \quad (6.4.12)$$

- For a cylindrical vessel breaking into two parts in a plane perpendicular to its axis:

$$v_i = 2.18a_0[F(L/R)^{1/2}]^{2/3} \quad (6.4.13)$$

where in F

$$\begin{aligned} A &= \pi r^2 & (\text{m}^2) \\ L &= \text{length of cylinder} & (\text{m}) \end{aligned}$$

- For a single small fragment ejected from a cylindrical vessel:

$$v_i = 2a_0 \left[\frac{Fs}{r} \right]^{0.38} \quad (6.4.14)$$

Equation (6.4.14) is only valid under the following conditions:

$$20 < P_v/P_0 < 300; \quad \gamma = 1.4; \quad s < 0.3r$$

- For the disintegration of both cylindrical and spherical vessels into multiple fragments:

$$v_i = 0.88a_0 F^{0.55} \quad (6.4.15)$$

6.4.2. Initial Fragment Velocity for Vessel Filled with Nonideal Gases

In many cases, pressurized gases in vessels do not behave as ideal gases. At very high pressures, van der Waals forces become important, that is, intermolecular forces and finite molecule size influence the gas behavior. Another nonideal situation is that in which, following the rupture of a vessel containing both gas and liquid, the liquid flashes.

Very little has been published covering such nonideal, but very realistic, situations. Two publications by Wiederman (1986a,b) treat nonideal gases. He uses a co-volume parameter, which is apparent in the Nobel–Abel equation of state of a nonideal gas, in order to quantify the influence on fragment velocity. The co-volume parameter is defined as the difference between a gas's initial-stage specific volume and its associated perfect gas value.

For a maximum value for the scaled pressure $\bar{p} = 0.1$, a reduction in v_i of 10% was calculated when the co-volume parameter was applied to a sphere breaking in half. In general, fragment velocity is lower than that calculated in the ideal-gas case. Baum (1987) recommends that energy E be determined from thermodynamic data (see Section 6.3.2.3) for the gas in question.

Wiederman (1986b) treats homogeneous, two-phase fluid states and some initially single-phase states which become homogeneous (single-state) during decompression. It was found that fragment hazards were somewhat more severe for a saturated-liquid state than for its corresponding gas-filled case. Maximum fragment velocities occurring during some limited experiments on liquid flashing could be calculated if 20% of the available energy, determined from thermodynamic data, was assumed to be kinetic energy (Baum 1987).

For vessels containing nonflashing liquids, the energy available for initial velocity can be determined by calculation of the energy contained in the gas. This value can be refined by taking into account the released energy of the expanding, originally compressed liquid.

6.4.3. Discussion

In Baum (1984), a comparison is made between the models described in Section 6.4.1. This comparison is depicted in Figure 6.35. The energy E was calculated with k according to Baum's refinement.

In Figure 6.35, lines have been added for a sphere bursting into 2 or 100 pieces for $p_1/p_0 = 50$ and 10, in accordance with Figure 6.33. Obviously, the simple relations proposed by Brode (1959) and Baum (1984) predict the highest velocity. Differences between models become significant for small values of scaled energy \bar{E} , in the following equation:

$$\bar{E} = [2E/(Ma_0^2)]^{1/2} \quad (6.4.16)$$

In most industrial applications, scaled energy will be between 0.1 and 0.4 (Baum 1984), so under normal conditions, few fragments are expected, and Figure 6.33 can be applied. However, if an operation or process is not under control and pressure rises dramatically, higher scaled-energy values can be reached.

In the relationships proposed by Brode (1959) and in Figure 6.33, velocity has no upper limit, although Figure 6.33 is approximately bounded by scaled pressures of 0.05 and 0.2 (scaled energies of approximately 0.1 and 0.7). Baum (1984) states, however, that there is an upper limit to velocity, as follows: The maximum velocity

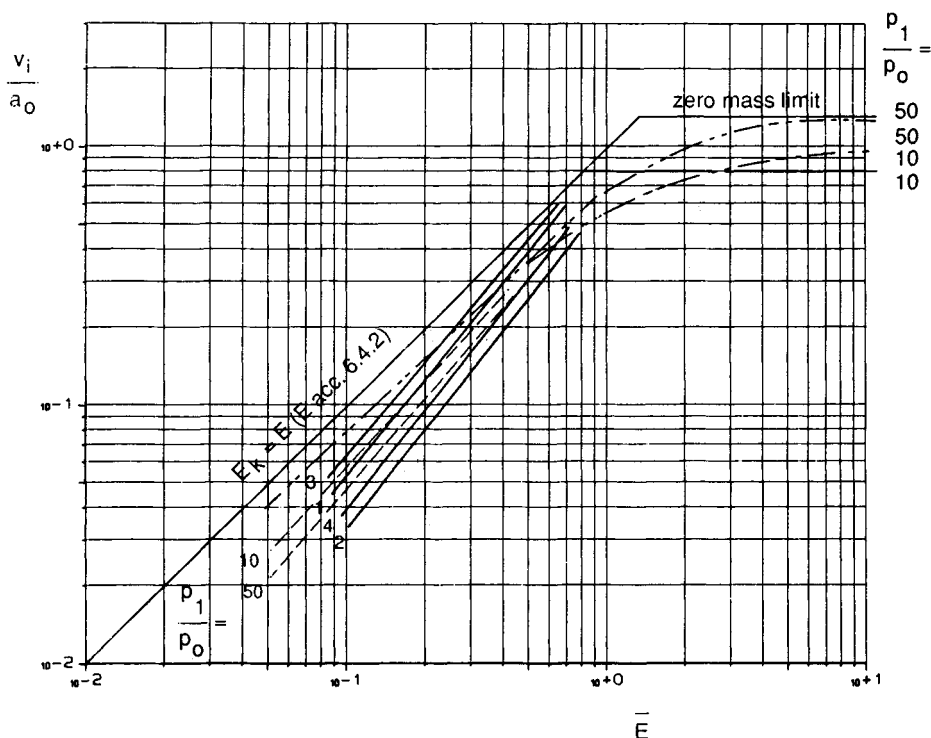


Figure 6.35. Calculated fragment velocities for a gas-filled sphere with $\gamma = 1.4$ (taken from Baum 1984; results of Baker et al. 1978a were added). (— —): Baum for $p_1/p_0 = 10$ and 50 . (— · —): Moore for $p_1/p_0 = 10$ and 50 . Baker: 1: $p_1/p_0 = 10$; number of fragments = 2
2: $p_1/p_0 = 50$; number of fragments = 2
3: $p_1/p_0 = 10$; number of fragments = 100
4: $p_1/p_0 = 50$; number of fragments = 100.

of massless fragments equals the maximum velocity of the expanding gas (the peak contact-surface velocity). In Figure 6.35, this maximum velocity is depicted by the horizontal lines for $p_1/p_0 = 10$ and 50 . If values in Figure 6.33 are extrapolated to higher scaled pressures, velocity will be overestimated.

The equation proposed by Moore (1967) tends to follow the upper-limit velocity. This is not surprising, because the equation was based upon high levels of energy. Despite its simplicity, its results compare fairly well with other models for both low and high energy levels.

For lower scaled pressures, velocity can be calculated with the equation proposed by Baum (1987) which produces disintegration of both cylindrical and spherical vessels into multiple fragments ($v_i = 0.88a_0F^{0.55}$). Such a result can also be obtained by use of Figure 6.33. However, actual experience is that ruptures rarely

produce a large number of fragments. The appearance of a large number of fragments in the low scaled-pressure regions of these equations or curves probably results from the nature of the laboratory tests from which the equations were derived. In those tests, small vessels made of special alloys were used; such alloys and sizes are not used in practice.

Baum's equation ($v_i = 0.88a_0F^{0.55}$) can be compared with curves in Figure 6.33 as F equals n times the scaled pressure, in which $n = 3$ for spheres and $n = 2$ for cylinders (end caps neglected). For spheres, Baum's equation gives higher velocities than the Baker et al. model (1983), but for cylinders, this equation gives lower velocities.

Note that work on ideal-gas-filled pressurized vessels, though extensive, is not complete. Furthermore, work on other cases, such as nonideal gases, flashing liquids, and gas plus loose particulate matter, has either just begun or not even begun. Because failure mode cannot be predicted accurately, the worst case must be assumed. The worst case may produce high calculated velocities and, consequently, large fragment ranges.

6.4.4. Ranges for Free Flying Fragments

After a fragment has attained a certain initial velocity, the forces acting upon it during flight are those of gravity and fluid dynamics. Fluid-dynamic forces are subdivided into drag and lift components. The effects of these forces depend on the fragment's shape and direction of motion relative to the wind.

6.4.4.1. Neglecting Dynamic Fluid Forces

The simplest relationship for calculating fragment range neglects drag and lift forces. Vertical and horizontal range, z_v and z_h , then depend upon initial velocity and initial trajectory angle α_i :

$$H = \frac{v_i^2 \sin(\alpha_i)^2}{2g} \quad (6.4.17)$$

$$R = \frac{v_i^2 \sin(2\alpha_i)}{g} \quad (6.4.18)$$

where

R	= horizontal range	(m)
H	= height fragment reaches	(m)
g	= gravitational acceleration	(m/s ²)
α_i	= initial angle between trajectory and a horizontal surface	(deg)
v_i	= initial fragment velocity	(m/s)

A fragment will travel the greatest horizontal distance when $\alpha_i = 45^\circ$.

$$R_{\max} = \frac{v_i^2}{g} \quad (6.4.19)$$

6.4.4.2. Incorporating Dynamic Fluid Forces

Incorporating the effects of fluid-dynamic forces requires the composition of a set of differential equations. Baker et al. (1983) plotted solutions of these equations in a diagram for practical use. They assumed that the position of a fragment during its flight remains the same with respect to its trajectory, that is, that the angle of attack remained constant. In fact, fragments probably tumble during flight. Plots of these calculations are given in Figure 6.36.

The figure plots scaled maximal range \bar{R} and scaled initial velocity \bar{v}_i given by

$$\bar{R} = \frac{\rho_0 C_D A_D R}{M_f} \quad (6.4.20)$$

$$\bar{v}_i = \frac{\rho_0 C_D A_D v_i^2}{M_f g} \quad (6.4.21)$$

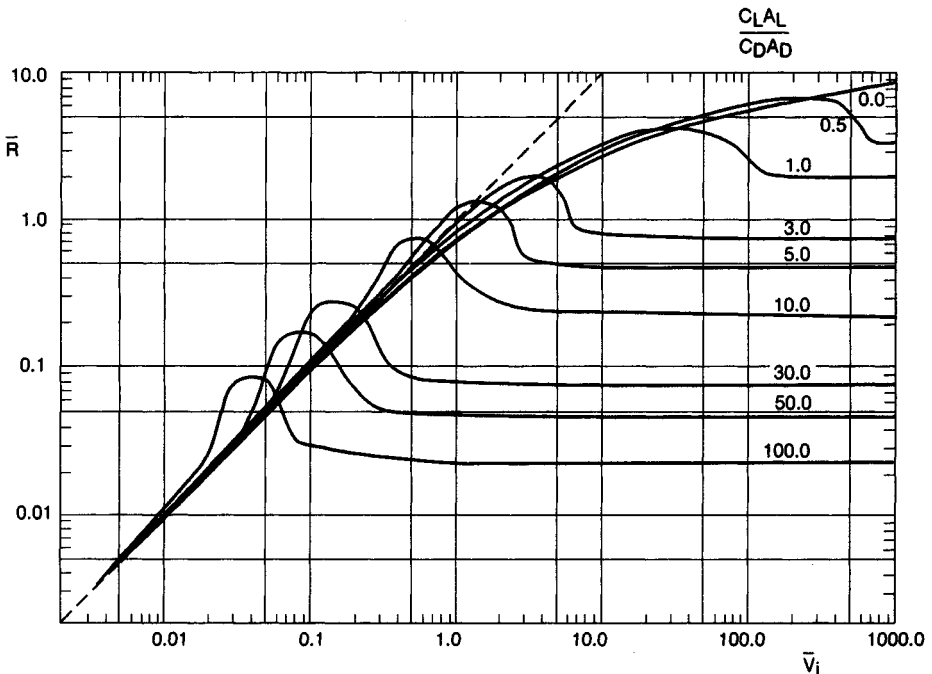


Figure 6.36. Scaled curves for fragment range predictions (taken from Baker et al. 1983) (— —): neglect of the fluid forces [Eq. (6.4.19)].

where

\bar{v}_i	= scaled initial velocity	(-)
\bar{R}	= scaled maximal range	(-)
R	= maximal range	(m)
ρ_0	= density of ambient atmosphere	(kg/m ³)
C_D	= drag coefficient	(-)
A_D	= exposed area in plane perpendicular to trajectory	(m ²)
g	= gravitational acceleration	(m/s ²)
M_f	= mass of fragment	(kg)

In Figure 6.36, two more parameters are used, namely

C_L	= lift coefficient	
A_L	= exposed area in plane parallel to trajectory	(m ²)

These curves were generated by maximization of range through variation of the initial trajectory angle. The curves are for similar lift-to-drag ratios $C_L A_L / (C_D A_D)$, so by varying the angle of attack (the angle between the fragment and the trajectory) for a certain fragment, the curve to be used changes. Furthermore, scaled velocity changes because drag area A_D changes, thus making Figure 6.36 difficult to interpret. A method of calculating drag-to-lift ratio is presented in Baker et al. (1983).

From Figure 6.36, it is clear that lifting force increases maximum range only in specific intervals of scaled velocity. In the case of thin plates, which have large $C_L A_L / (C_D A_D)$ ratios, the so-called "frisbeeing" effect occurs, and the scaled range more than doubles the range calculated when fluid forces are neglected.



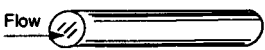
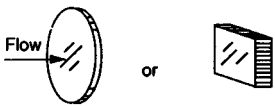
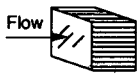
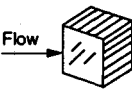
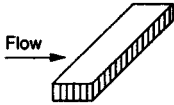
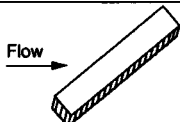

The dotted line in the curve denotes the case for which fluid dynamic forces are neglected $R_{\max} = v_i^2/g$ [Eq. (6.4.19)]. In most cases, "chunky" fragments are expected. The lift coefficient will be zero for these fragments, so only drag and gravity will act on them; the curve with $C_L A_L / (C_D A_D) = 0$ is then valid. Drag force becomes significant for scaled velocities greater than 1. Drag coefficients for various shapes can be found in Table 6.13. More information about lift and drag can be found in Hoerner (1958).

For fragments having plate-like shapes, the lift forces can be large, so predicted ranges can be much larger than the range calculated with $R_{\max} = v_i^2/g$, especially when the angle of attack α_i is small ($\alpha_i =$ approximately 10°). The sensitivity of the angle of attack model is high, however. For example, an angle of attack of zero results in no lift force at all.

6.4.5. Ranges for Rocketing Fragments

Some accidents involving materials like propane and butane resulted in the propulsion of large fragments for unexpectedly long distances. Baker et al. (1978b) argued that these fragments developed a "rocketing" effect. In their model, a fragment

TABLE 6.13. Drag Coefficients (Baker et al. 1983)

SHAPE	SKETCH	C_D
Right Circular Cylinder (long rod), side-on		1.20
Sphere		0.47
Rod, end-on		0.82
Disc, face-on		1.17
Cube, face-on		1.05
Cube, edge-on		0.80
Long Rectangular Member, face-on		2.05
Long Rectangular Member, edge-on		1.55
Narrow Strip, face-on		1.98

retains a portion of the vessel's liquid contents. Liquid vaporizes during the initial stage of flight, thereby accelerating the fragment as vapor escapes through the opening. Baker et al. (1978b) provided equations for a simplified rocketing problem and a computer program for their solution, but stated that the method was not yet ready to be used for range prediction. Baker et al. (1983) applied this method to two cases, and compared predicted and actual ranges of assumed rocketed fragments. This approach may be applicable to similar cases; otherwise, the computer program should be employed.

Ranges for rocketing fragments can also be calculated from guidelines given by Baum (1987). As stated in Section 6.4.2, for cases in which liquid flashes off, the initial-velocity calculation must take into account total energy. If this is done, rocketing fragments and fragments from a bursting vessel in which liquid flashes are assumed to be the same.

Ranges were calculated for a simulated accident with the methods of Baker et al. (1978a,b) and Baum (1987). It appears that the difference between these approaches is small. Initial trajectory angle has a great effect on results. In many cases (e.g., for horizontal cylinders) a small initial trajectory angle may be expected. If, however, the optimal angle is used, very long ranges are predicted.

6.4.6. Statistical Analysis of Fragments from Accidental Explosions

Theoretical models presented in previous sections give no information on distributions of mass, velocity, or range of fragments, and very little information on the number of fragments to be expected. Apparently, these models are not developed sufficiently to account for these parameters. More information can probably be found in the analysis of results of accidental explosions. It appears, however, that vital information is lacking for most such events.

Baker (1978b) analyzed 25 accidental vessel explosions for mass and range distribution and fragment shape. This statistical analysis is considered the most complete in the open literature. Because data on most of the 25 events considered in the analysis were limited, it was necessary to group like events into six groups in order to yield an adequate base for useful statistical analysis.

Information on each group is tabulated in Table 6.14. The values for energy range in Table 6.14 require some discussion. In the reference, all energy values were calculated by use of Eq. (6.4.2). Users should do the same in order to select the right event group. Furthermore, some energy values given are rather low; it is doubtful that they are correct.

Statistical analyses were performed on each of the groups to yield, as data availability permitted, estimates of fragment-range distributions and fragment-mass distributions. The next sections are dedicated to the statistical analysis according to the Baker et al. (1978b) method.

TABLE 6.14. Groups of Like Events

<i>Event Group Number</i>	<i>Number of Events</i>	<i>Explosion Material</i>	<i>Source Energy Range (J)</i>	<i>Vessel Shape</i>	<i>Vessel Mass (kg)</i>	<i>Number of Fragments</i>
1	4	Propane, Anhydrous ammonia	1.487×10^5 to 5.95×10^5	Railroad tank car	25,542 to 83,900	14
2	9	LPG	3814 to 3921.3	Railroad tank car	25,464	28
3	1	Air	5.198×10^{11}	Cylinder pipe and spheres	145,842	35
4	2	LPG, Propylene	549.6	Semi-trailer (cylinder)	6343 to 7840	31
5	3	Argon	2438×10^9 to 1133×10^{10}	Sphere	48.26 to 187.33	14
6	1	Propane	24.78	Cylinder	511.7	11

6.4.6.1. *Fragment Range Distribution*

It was shown in the reference that the fragment range distribution for each of the six groups of events follows a normal, or Gaussian, distribution. It was then shown that the chosen distributions were statistically acceptable. The range distributions for each group are given in Figures 6.37a and 6.37b. With this information, it is possible to determine the percentage of all the fragments which would have a range smaller than, or equal to, a certain value. Table 6.15 gives an overview of statistical results for each event group.

6.4.6.2. *Fragment-Mass Distribution*

Pertinent fragment-mass distributions were available on three event groups (2, 3, and 6). According to the reference, they follow a normal, or Gaussian, distribution. These distributions are presented in Figures 6.38 and 6.39. As with the information in Figures 6.37a and 6.37b, the percentage of fragments having a mass smaller than or equal to a certain value can be calculated. Table 6.16 gives a statistical summary for event groups 2, 3, and 6.

6.5. SUMMARY AND DISCUSSION

It should now be clear that there are a number of unsolved problems with regard to BLEVEs. These problems are summarized in this section.

With regard to radiation:

- Additional experiments should be performed on a large scale to establish the emissive power of fireballs generated by BLEVEs. The effects of flammable substances involved, fireball diameter, and initial pressure should be investigated.
- Such experiments should also determine the influences of fill ratio, pressure, substance, and degree of superheat on mass contributing to fireball generation.

With regard to overpressure generation:

- It is not clear which measure of explosion energy is most suitable. Note that, in the method presented in Section 6.3, the energy of gas-filled pressure vessel bursts is calculated by use of Brode's formula, and for vessels filled with vapor, by use of the formula for work done in expansion.
- Blast parameters for surface bursts of gas-filled pressure vessels have not been investigated thoroughly. Parameters presently used are derived from investigations of free-air bursts.

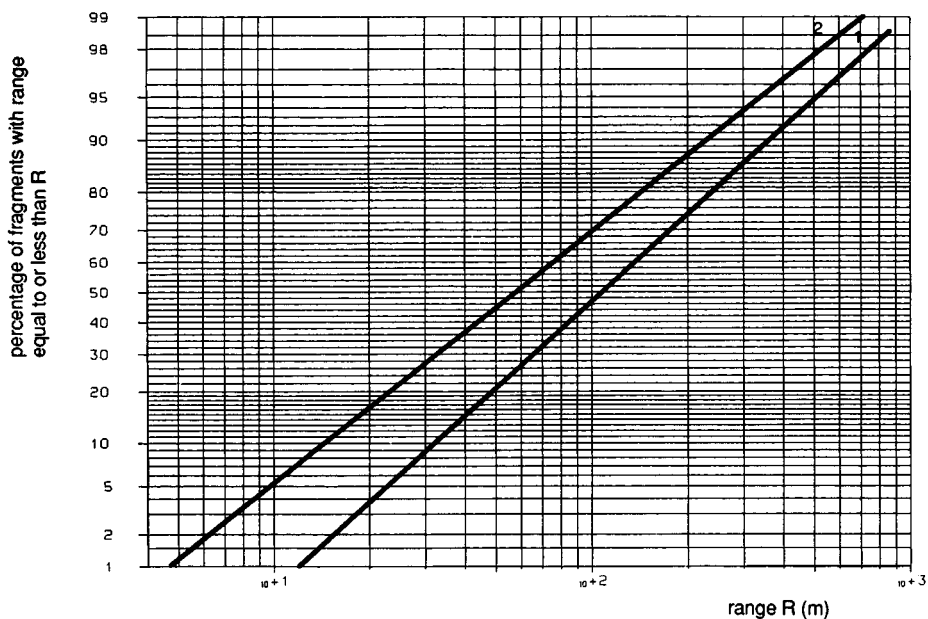


Figure 6.37a. Fragment range distribution for event groups 1 and 2 (Baker et al. 1978b).

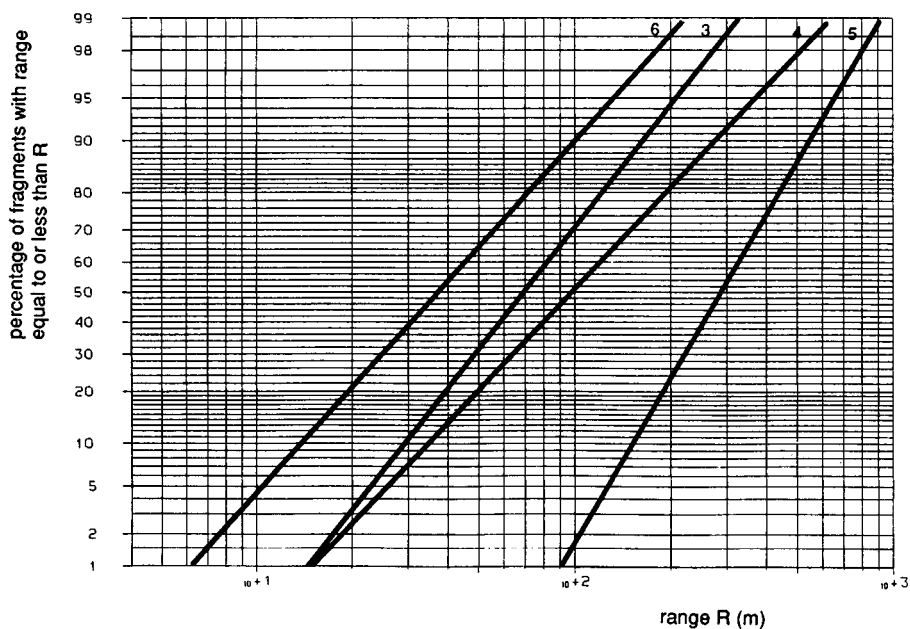


Figure 6.37b. Fragment range distribution for event groups 3, 4, 5, and 6 (Baker et al. 1978b).

TABLE 6.15. Estimated Means and Standard Deviations for Log-Normal Range Distributions (base *e*) for Six Event Groups

Event Group	Estimated Mean	Estimated Standard Deviation
1	4.57	0.91
2	4.10	1.06
3	4.28	0.65
4	4.63	0.79
5	5.66	0.45
6	3.67	0.76

- The influence of nonspherical releases (e.g., burst of a cylindrical vessel, jetting) on blast parameters has not been thoroughly investigated.
- Reid’s theory that a superheated liquid which flashes below its homogeneous nucleation temperature T_{sl} will not give rise to strong blast generation has not been verified.

With regard to missiles:

- The fraction of explosion energy which contributes to fragment generation is unclear. Its effect on initial fragment velocity deserves more attention in relation

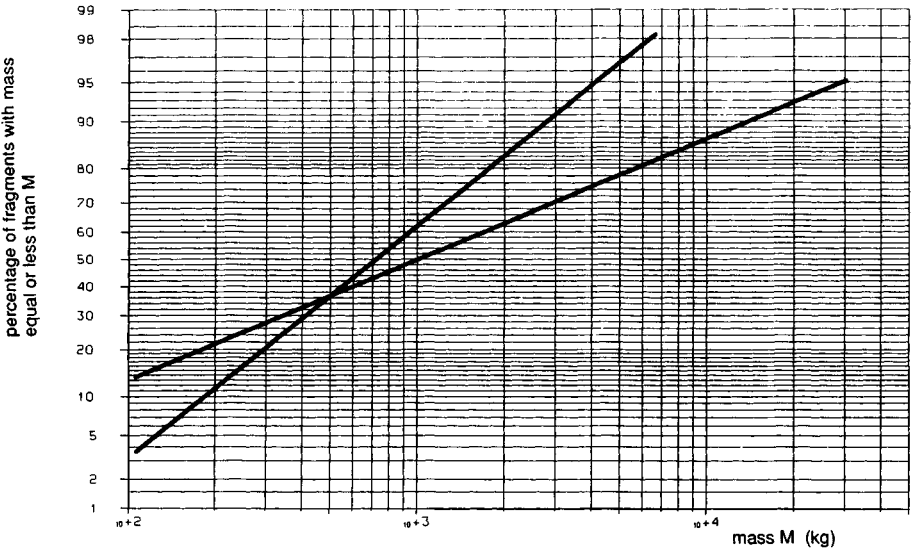


Figure 6.38. Fragment-mass distribution for event groups 2 and 3 (Baker et al. 1978b).

TABLE 6.16. Estimated Means and Standard Deviations for Log-Normal Range Distributions (base e) for Event-Groups 2, 3, and 6

Event Group	Estimated Mean	Estimated Standard Deviation
2	7.05	2.12
3	6.62	1.05
6	1.42	2.78

to such factors as conditions within the vessel and properties of the vessel's materials.

- Methods do not exist to predict even the order of magnitude of the number of fragments produced. One assumes failure either into two parts or into a large number of fragments. The effect of parameters such as material, wall thickness, and initial pressure are not known.

REFERENCES

Adamczyk, A. A. 1976. An investigation of blast waves generated from non-ideal energy sources. *UILU-ENG 76-0506*. Urbana: University of Illinois.

American Petroleum Institute. 1982. Recommended Practice 521.

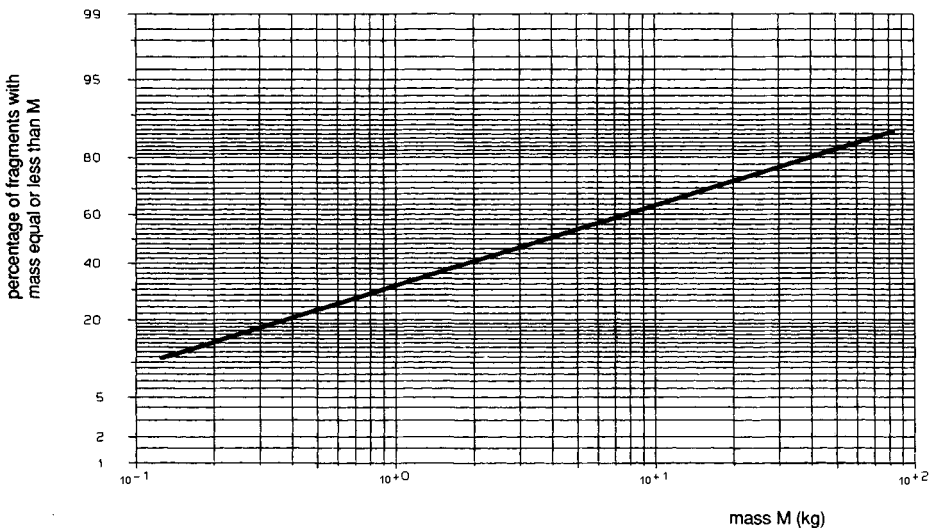


Figure 6.39. Fragment-mass distribution for event group 6.

- Anderson, C., W. Townsend, R. Markland, and J. Zook. 1975. Comparison of various thermal systems for the protection of railroad tank cars tested at the FRA/BRL torching facility. Interim Memorandum Report No. 459, Ballistic Research Laboratories.
- Aslanov, S. K., and O. S. Golinskii. 1989. Energy of an asymptotically equivalent point detonation for the detonation of a charge of finite volume in an ideal gas. *Combustion, Explosion, and Shock Waves*, pp. 801–808.
- Bader, B. E., A. B. Donaldson, and H. C. Hardee. 1971. Liquid-propellant rocket abort fire model. *J. Spacecraft and Rockets* 8:1216–1219.
- Baker, W. E. 1973. *Explosions in Air*. Austin: University of Texas Press.
- Baker, W. E., J. J. Kulesz, R. E. Richer, R. L. Bessey, P. S. Westine, V. B. Parr, and G. A. Oldham. 1975 and 1977. *Workbook for Predicting Pressure Wave and Fragment Effects of Exploding Propellant Tanks and Gas Storage Vessels*. NASA CR-134906. Washington: NASA Scientific and Technical Information Office.
- Baker, W. E., J. J. Kulesz, P. A. Cox, P. S. Westine, and R. A. Strehlow. 1978a. *A Short Course on Explosion Hazards Evaluation*. Southwest Research Institute.
- Baker, W. E., J. J. Kulesz, R. E. Richer, P. S. Westine, V. B. Parr, L. M. Vargas, and P. K. Moseley. 1978b. *Workbook for Estimating the Effects of Accidental Explosions in Propellant Handling Systems*. NASA CR-3023. Washington: NASA Scientific and Technical Information Office.
- Baker, W. E., P. A. Cox, P. S. Westine, J. J. Kulesz, and R. A. Strehlow. 1983. Explosion Hazards and Evaluation. In *Fundamental Studies in Engineering*, Vol. 5. New York: Elsevier.
- Baum, M. R. 1984. The velocity of missiles generated by the disintegration of gas pressurized vessels and pipes. *Trans. ASME*. 106:362–368.
- Baum, M. R. 1987. Disruptive failure of pressure vessels: preliminary design guide lines for fragment velocity and the extent of the hazard zone. In *Advances in Impact, Blast Ballistics, and Dynamic Analysis of Structures*. ASME PVP. 124. New York: ASME.
- Bessey, R. L. 1974. Fragment velocities from exploding liquid propellant tanks. *Shock Vibrat. Bull.* 44.
- Bessey, R. L., and J. J. Kulesz. 1976. Fragment velocities from bursting cylindrical and spherical pressure vessels. *Shock Vibrat. Bull.* 46.
- Board, S. J., R. W. Hall, and R. S. Hall. 1975. Detonation of fuel coolant explosions. *Nature* 254:319–320.
- Boyer, D. W., H. L. Brode, I. I. Glass, and J. G. Hall. 1958. "Blast from a pressurized sphere." UTIA Report No. 48. Toronto: Institute of Aerophysics, University of Toronto.
- Brode, H. L. 1955. Numerical solutions of spherical blast waves. *J. Appl. Phys.* 26:766–775.
- Brode, H. L. 1959. Blast wave from a spherical charge. *Phys. Fluids*. 2:217.
- Center for Chemical Process Safety. 1989. *Guidelines for Chemical Process Quantitative Risk Analysis*. New York: AIChE/CCPS.
- Chushkin, P. I., and L. V. Shurshalov. 1982. Numerical computations of explosions in gases. (Lecture Notes in Physics 170). *Proc. 8th Int. Conf. on Num. Meth. in Fluid Dynam.*, 21–42. Berlin: Springer Verlag.
- Droste, B., and W. Schoen. 1988. Full-scale fire tests with unprotected and thermal insulated LPG storage tanks. *J. Haz. Mat.* 20:41–53.
- Edmister, W. C., and B. I. Lee. 1984. *Applied Hydrocarbon Thermodynamics*, 2nd ed. Houston: Gulf Publishing Company.
- Esparza, E. D., and W. E. Baker. 1977a. *Measurement of Blast Waves from Bursting Pressurized Frangible Spheres*. NASA CR-2843. Washington: NASA Scientific and Technical Information Office.

- Esparza, E. D., and W. E. Baker. 1977b. *Measurement of Blast Waves from Bursting Frangible Spheres Pressurized with Flash-evaporating Vapor or Liquid*. NASA CR-2811. Washington: NASA Scientific and Technical Information Office.
- Fay, J. A., and D. H. Lewis, Jr. 1977. Unsteady burning of unconfined fuel vapor clouds. *Sixteenth Symposium (International) on Combustion*, 1397–1404. Pittsburgh: The Combustion Institute.
- Giesbrecht, H., K. Hess, W. Leuckel, and B. Maurer. 1980. Analyse der potentiellen Explosionswirkung von kurzzeitig in de Atmosphaere freigesetzten Brenngasmengen. *Chem. Ing. Tech.* 52(2):114–122.
- Glass, I. I. 1960. *UTIA Report No. 58*. Toronto: Institute of Aerophysics, University of Toronto.
- Glasstone, S. 1957. The effects of nuclear weapons. USAEC.
- Grodzovskii, G. L., and F. A. Kukanov. 1965. Motions of fragments of a vessel bursting in a vacuum. *Inzhenemyi Zhurnal* 5(2):352–355.
- Guirao, C. M., and G. G. Bach. 1979. On the scaling of blast waves from fuel–air explosives. *Proc. 6th Symp. Blast Simulation*. Cahors, France.
- Hardee, H. C., and D. O. Lee. 1973. Thermal hazard from propane fireballs. *Trans. Plan. Tech.* 2:121–128.
- Hardee, H. C., and D. O. Lee. 1978. A simple conduction model for skin burns resulting from exposure to chemical fireballs. *Fire Res.* 1:199–205.
- Hardee, H. C., D. O. Lee, and W. B. Benedict. 1978. Thermal hazards from LNG fireballs. *Combust. Sci. Tech.* 17:189–197.
- Hasegawa, K., and K. Sato. 1977. Study on the fireball following steam explosion of *n*-pentane. *Second Int. Symp. on Loss Prevention and Safety Promotion in the Process Ind.*, pp. 297–304. Heidelberg.
- Hasegawa, K., and K. Sato. 1987. Experimental investigation of unconfined vapor cloud explosions and hydrocarbons. Technical Memorandum No. 16, Fire Research Institute, Tokyo.
- High, R. 1968. The Saturn fireball. *Ann. N.Y. Acad. Sci.* 152:441–451.
- Hoerner, S. F. 1958. *Fluid Dynamic Drag*. Midland Park, NJ: Author.
- Hymes, J. 1983. The physiological and pathological effects of thermal radiation. *SRD R 275*. U.K. Atomic Energy Authority.
- Jaggers, H. C., O. P. Franklin, D. R. Wad, and F. G. Roper. 1986. Factors controlling burning time for non-mixed clouds of fuel gas. *I. Chem. E. Symp. Ser.* No. 97.
- Johansson, O. 1986. BLEVES à San Juanico. *Face au Risque*. 222(4):35–37, 55–58.
- Johnson, D. M., M. J. Pritchard, and M. J. Wickens. 1990. Large scale catastrophic releases of flammable liquids. Commission of the European Communities Report, Contract No.: EV4T.0014.UK(H).
- Lewis, D. 1985. New definition for BLEVES. *Haz. Cargo Bull.* April, 1985: 28–31.
- Liepmann, H. W., and A. Roshko. 1967. *Elements of Gas Dynamics*. New York: John Wiley and Sons.
- Lihou, D. A., and J. K. Maund. 1982. Thermal radiation hazard from fireballs. *I. Chem. E. Symp. Ser.* No. 71, pp. 191–225.
- Maurer, B., K. Hess, H. Giesbrecht, and W. Leuckel. 1977. Modeling vapor cloud dispersion and deflagration after bursting of tanks filled with liquefied gas. *Second Int. Symp. on Loss Prevention and Safety Promotion in the Process Ind.*, pp. 305–321. Heidelberg.
- McDevitt, C. A., F. R. Steward, and J. E. S. Venart. 1987. What is a BLEVE? *Proc. 4th Tech. Seminar Chem. Spills*, pp. 137–147. Toronto.

- Moodie, K., L. T. Cowley, R. B. Denny, L. M. Small, and I. Williams. 1988. Fire engulfment tests on a 5-ton tank. *J. Haz. Mat.* 20:55–71.
- Moore, C. V. 1967. *Nucl. Eng. Des.* 5:81–97.
- Moorhouse, J., and M. J. Pritchard. 1982. Thermal radiation from large pool fires and thermals—literature review. *I. Chem. E. Symp. Series* No. 71.
- Moskowitz, H. 1965. AIAA paper no. 65–195.
- Mudan, K. S. 1984. Thermal radiation hazards from hydrocarbon pool fires. *Progr. Energy Combust. Sci.* 10(1):59–80.
- Opschoor, G. 1974. Onderzoek naar de explosieve verdamping van op water uitspreidend LNG. Report Centraal Technisch Instituut TNO, Ref. 74-03386.
- Pape, R. P., et al. (Working Group, Thermal Radiation), 1988. Calculation of the intensity of thermal radiation from large fires. *Loss Prev. Bull.* 82:1–11.
- Perry, R. H., and D. Green. 1984. *Perry's Chemical Engineers' Handbook*, 6th ed. New York: McGraw-Hill.
- Pietersen, C. M. 1985. Analysis of the LPG incident in San Juan Ixhuatepec, Mexico City, 19 November 1984. Report TNO Division of Technology for Society, 1985.
- Pitblado, R. M. 1986. Consequence models for BLEVE incidents. Major Industrial Hazards Project, NSW 2006. University of Sydney.
- Pittman, J. F. 1972. *Blast and Fragment Hazards from Bursting High Pressure Tanks*. NOLTR 72-102. Silver Spring, Maryland: U.S. Naval Ordnance Laboratory.
- Pittman, J. F. 1976. *Blast and Fragments from Superpressure Vessel Rupture*. NSWC/WOL/TR 75–87. White Oak, Silver Spring, Maryland: Naval Surface Weapons Center.
- Raj, P. K. 1977. Calculation of thermal radiation hazards from LNG fires. *A Review of the State of the Art, AGA Transmission Conference T135–148*.
- Raju, M. S., and R. A. Strehlow. 1984. Numerical Investigations of Nonideal Explosions. *J. Haz. Mat.* 9:265–290.
- Reid, R. C. 1976. Superheated liquids. *Amer. Scientist.* 64:146–156.
- Reid, R. C. 1979. Possible mechanism for pressurized-liquid tank explosions or BLEVE's. *Science.* 203(3).
- Reid, R. C. 1980. Some theories on boiling liquid expanding vapor explosions. *Fire*. March 1980: 525–526.
- Roberts, A. F. 1982. Thermal radiation hazards from release of LPG fires from pressurized storage. *Fire Safety J.* 4:197–212.
- Schmidli, J., S. Banerjee, and G. Yadigaroglu. 1990. Effects of vapor/aerosol and pool formation on rupture of vessel containing superheated liquid. *J. Loss Prev. Proc. Ind.* 3(1):104–111.
- Schoen, W., U. Probst, and B. Droste. 1989. Experimental investigations of fire protection measures for LPG storage tanks. *Proc. 6th Int. Symp. on Loss Prevention and Safety Promotion in the Process Ind.* 51:1–17.
- Schulz-Forberg, B., B. Droste, and H. Charlett. 1984. Failure mechanics of propane tanks under thermal stresses including fire engulfment. *Proc. Int. Symp. on Transport and Storage of LPG and LNG.* 1:295–305.
- Stoll, A. M., and M. A. Chianta. 1971. *Trans. N.Y. Acad. Sci.*, 649–670.
- Taylor, D. B., and C. F. Price. 1971. Velocity of Fragments from Bursting Gas Reservoirs. *ASME Trans. J. Eng. Ind.* 93B:981–985.
- Van Wees, R. M. 1989. Explosion Hazards of Storage Vessels: Estimation of Explosion Effects. TNO-Prins Maurits Laboratory Report No. PML 1989-C61. Rijswijk, The Netherlands.

- Venart, J. E. S. 1990. The Anatomy of a Boiling Liquid Expanding Vapor Explosion (BLEVE). *24th Annual Loss Prevention Symposium*. New Orleans, May 1990.
- Walls, W. L. 1979. The BLEVE—Part 1. *Fire Command*. May 1979: 22–24. The BLEVE—Part 2. *Fire Command*. June 1979: 35–37.
- Wiederman, A. H. 1986a. Air-blast and fragment environments produced by the bursting of vessels filled with very high pressure gases. In *Advances in Impact, Blast Ballistics, and Dynamic Analysis of Structures*. ASME PVP. 106. New York: ASME.
- Wiederman, A. H. 1986b. Air-blast and fragment environments produced by the bursting of pressurized vessels filled with two phase fluids. In *Advances in Impact, Blast Ballistics, and Dynamic Analysis of Structures*. ASME PVP. 106. New York: ASME.
- Williamson, B. R., and L. R. B. Mann. 1981. Thermal hazards from propane (LPG) fireballs. *Combust. Sci. Tech.* 25:141–145.